Finger Motion Modeling for Bionic Fingers

Myrielle Allen-Prince and Dr. Jay Walton

July 2011

Abstract

The use of bionic hands is becoming a reality for those who have suffered amputation. Mathematical models are necessary to calculate the forces needed on each tendon to mimic the motion of human fingers. We modeled the motion of the human finger and thumb as it bends in and out using Newton's second law of motion. A system of partial differntial equations was developed to describe the relationship of the forces needed to move the finger to a specified position, incorporating a feedback mechanism. Our work shows that this type of model can be used to accurately control the motion of a human finger.

1 Introduction

In the United States alone, approximately 1.7 million have suffered a limb loss between 1988 and 1996. In fact, about one out of every 200 people in the United States has had an amputation [1]. Amputation rates may be on the increase dut to the epidemic of diabetes in the United States. Many of those amputees look for ways to regain the use or their limbs via prostheses.

Bionic limbs are mechanically engineered prostheses which are used to give the person mobility and movement in the limb that was missing. Finding ways to duplicate the motion of the human body is crucial to the development of bionic prostheses. In 1999, Baek et. al. developed a simple model for a robotic finger [2]. In 2008, Arslan et. al. focused on a biomechanical model of the index finger of the human hand which was based on human anatomy. Because activation of a finger is done through tendons, they used a tendon configuration to imitate the characteristics and functionality of the human hand [4].

Mimicking the exact functions of the hand is extremely complex because of the free range of motion of the fingers and thumb. We modeled a simplified motion of the finger using Newton's second law of motion.

2 Method

A phalanx is the section of the finger between each joint so each finger, other than the thumb, has three phalanges. Phalanx 1 is the secton closest to the palm. Figure 1 shows the forces, mass, and angles involved in the movement of the phalanges of a finger. The radius of the joint at the base of the ith phalanx is represented by r_i. The angle between the horizontal and the center of the phalanx is θ_i, L_i is the length of the phalanx, m_i the center of mass of the ith phalanx, and $T(\theta_i)$ the tension force at the center of mass of the ith phalanx. We used an idealized mechanical model in which each phalange is assumed

to be infinitely rigi
center of mass of e
idealizations of ten

We assumed th
in a circular motic
assumed to be rigic
on the mass m_1 affe
involving circular r

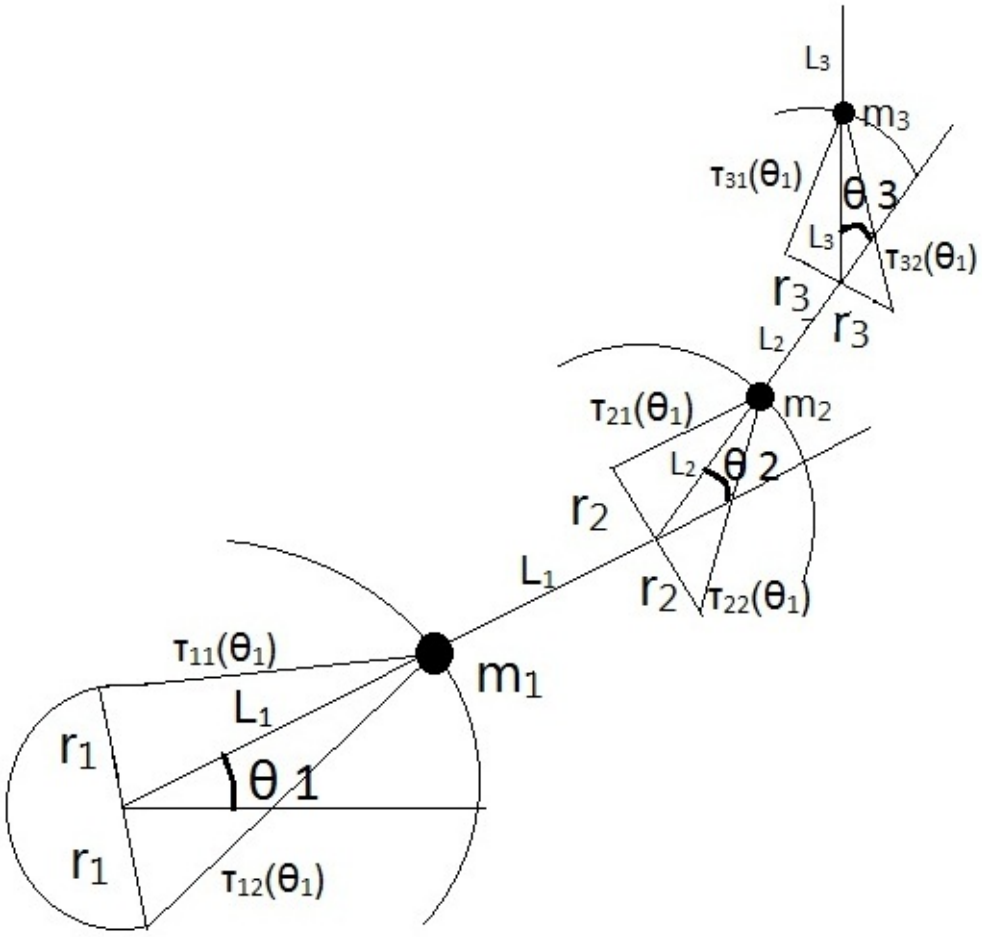

Figure 1: Diagram of Finger

The force and acceleration equations are shown below. Force on m_1:

$$F_1 = \sin(\alpha_1)(T_{11} - T_{12}) - \sin(\theta_2 - \theta_1)(\cos(\alpha_2)(T_{21} + T_{22}) + \cos(\alpha_3)\cos(\theta_3 - \theta_2)(T_{31} + T_{32}))$$

Force on m_2:

$$F_2 = \sin(\alpha_2)(T_{21} - T_{22}) - \sin(\theta_3 - \theta_2)(\cos(\alpha_3)(T_{31} + T_{32})$$

Force on m_3:

$$F_3 = \sin(\alpha_3)(T_{31} - T_{32})$$

Acceleration of m_1:

$$\ddot{u}_1 = \tau_1(\theta_1)L_1\ddot{\theta}_1$$

Acceleration of m_2:

$$\ddot{u}_2 = \tau_2(\theta_2)(2L_1\cos(\theta_2 - \theta_1)\ddot{\theta}_1 + 2L_1\sin(\theta_2 - \theta_1)(\dot{\theta}_1)^2 + L_2\ddot{\theta}_2)$$

Acceleration of m_3:

$$\ddot{u}_3 \cdot \tau_3'(\theta_3) = 2L_1(\cos(\theta_3 - \theta_1)\ddot{\theta}_1 + \sin(\theta_3 - \theta_1)(\dot{\theta})^2) + 2L_2(\cos(\theta_3 - \theta 2)\ddot{\theta}_2 + \sin(\theta_3 - \theta_2)(\dot{\theta}_2)^2) + L_3\ddot{\theta}_3$$

Multiplying the acceleration by mass and then equating with force gives the system of equations below.

$$m_1L_1\ddot{\theta}_1 = \sin(\alpha_1)(T_{11} - T_{12}) - \sin(\theta_2 - \theta_1)(\cos(\alpha_2)(T_{21} + T_{22}) + \cos(\alpha_3)\cos(\theta_3 - \theta_2)(T_{31} + T_{32})) \quad (1)$$

$$2L_1 \cos(\theta_2 - \theta_1)\ddot{\theta}_1 + 2L_1 \sin(\theta_2 - \theta_1)(\dot{\theta}_1)^2 + L_2\ddot{\theta}_2 = \tag{2}$$

$$\sin(\alpha_2)(T_{21} - T_{22}) - (\cos(\alpha_3)(T_{31} + T_{32}) \sin(\theta_3 - \theta_2)) \tag{3}$$

$$\tag{4}$$

$$m_3(\ddot{u}_3 \cdot \tau_3'(\theta_3)) = (F_3 \cdot \tau_3(\theta_3)) \tag{5}$$

Numerical solutions of these partial differential equations were obtained in Mathematica using numerical method of lines [3]. Given each length L_i and each function $\theta_i(t)$, one can appeal to Figure 1 to graph the trajectory of the idealized mechanical finger.

3 Results

Figure 2 shows an example of the motion of the finger according to this model. The tendon forces for this example are

$$\begin{aligned} T_{11}(t) &= (t/(1+t))(0.0044) \\ T_{12}(t) &= 0 \\ T_{21}(t) &= (t/(1+t))(0.00989) \end{aligned}$$

wit
α_i =

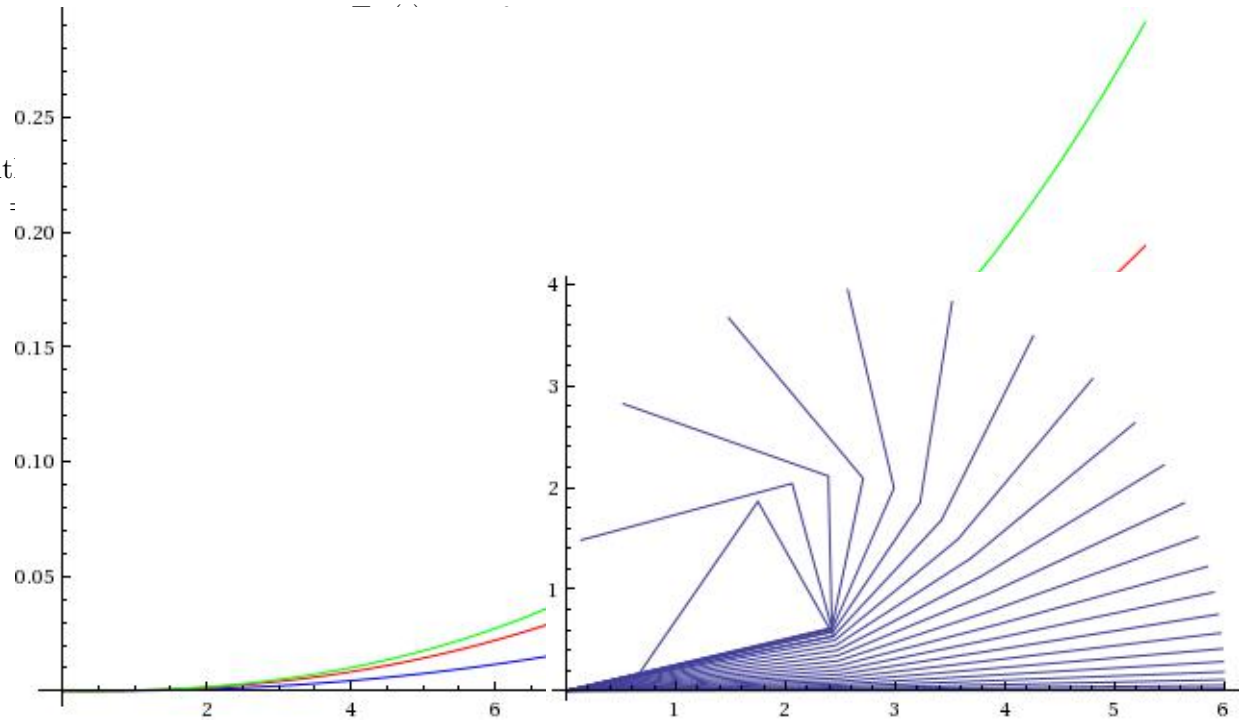

Figure 2: Finger motion. Left: one curve per phalange, with time t on the horizontal axis and angle θ on the vertical axis. Right: one curve per time unit $t = 1 \ldots 23$, with x position on the horizontal axis and y position on the vertical axis.

To get a different outcome, we had to repeatedly adjust the forces. It was observed in simulations that the predicted trajectories were rather sensitive to the relationships among the applied forces which at times caused a severe hyperextension of one or more joints. This can occur from allowing the force of the first phalanx to exceed the second or the second

to exceed the third. In the case of figure 3, the force on the second phalanx was lower than the force on the first phalanx.

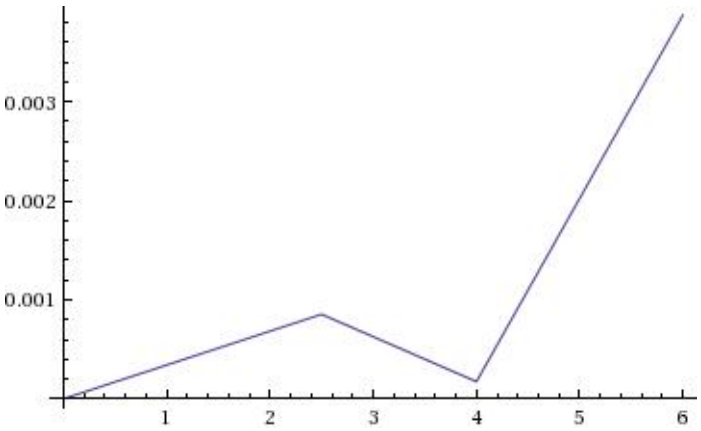

Figure 3: Hyperextended joint.

In Mathematica, we were able to graph the actual form of the the finger and capture its motion as it curves in time. Figure 2 shows the finger as $t = [1 - 23]$, but is unrealistic for most because the third phalanx has an excessive bend. This bend can not physically occur without more bending in the first and second phalanx.

In order to get a more realistic bend, more realistic parameters had to be used. The initial parameters for the length of each phalanx was 1 in. for L_1, 0.9 in. for L_2, and 0.5 in. for L_3. We changed these to 1.25 in, 0.75 in. and 1 in. allowing better curves. The measurements were taken from the inside of the finger at the creases, which causes the length of the third phalanx to be slightly greater than the second.

Figure 4 shows the thumb with the paramters $m_1 = 1$ and $m_2 = .9$, $L_1 = 1.5$ and $L_2 = 1.375$, and $\alpha_1 = \Pi/4.0$ and $\alpha_2 = \Pi/4.0$. The angles θ_i was subtracted from $\pi/2$ to get the correct placement corresponding to an actual hand. One challenge that was addressed was how to use this mechanical model to mimic the feedback mechanism provided by human vision to dynamically adjust the forces in a hand to cause the finger and thumb to touch. This feedback loop was simulated by initially selecting a distribution of forces which were applied until the ends of the finger and thumb ceased to move closer to one another. At that time the forces were adjusted until the finger and thumb began to move closer again. If they began to diverge at some later time, the simulation was stopped, forces readjusted, and the simulation restarted. This process was continued until the thumb and the finger was successfully brought together as in figure 5.

4 Conclusion

What was accomphlished in this study was the essential first step of developing and simulating a mathematical model of the motion of a finger and thumb mechanical system. The next very challenging task is to devise a mathematical theory for controlling the action of this mechanical system from visual feedback.

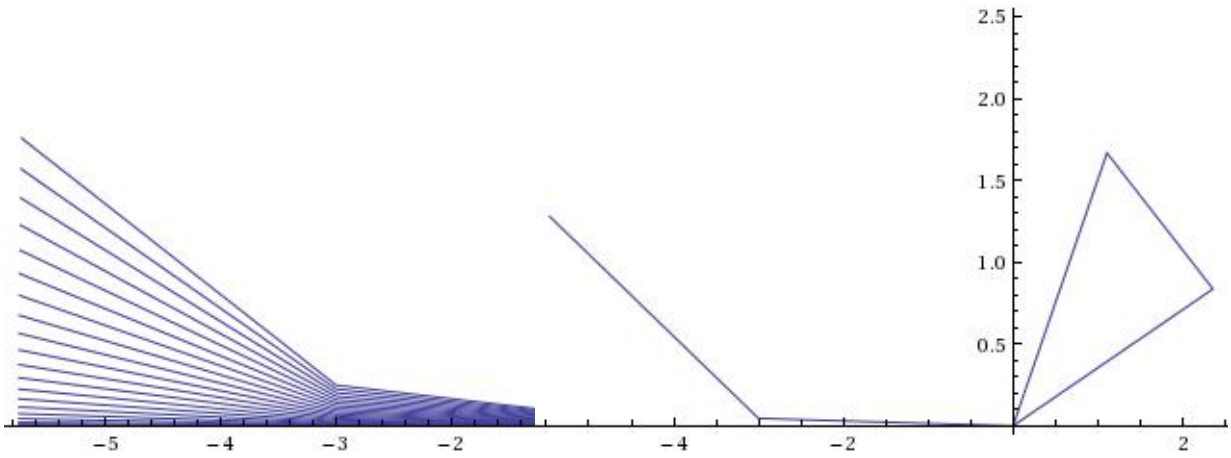

Figure 4: Thumb-Finger. Left: one curve per time unit $t = 1 \dots 23$,with x position on the horizontal axis and y position on the vertical axis. Right: curve on $-x$ horizontal axis for the thumb and curve on x horizontal axis for the finger, both at $t = 23$ with x position on the horizontal axis and y position on the vertical axis.

References

[1] National Limb Loss Information Center. Amputation statistics by cause limb loss in the united states. http://www.amputee-coalition.org/fact_sheets/amp_stats_cause.html, 2008.

[2] J. H. Chang S. E. Baek, S. H. Lee. Design and control of a robotic finger for prosthetic hands. *Proceedings of the 1999 IEEE/RSJ International Conference on Intelligent Robots and Systems*, pages 113--117, 1999.

[3] Inc. Wolfram Research. Mathematica edition: Version 8.0. Wolfram Research, Inc., Champaign, Illinois, 2010.

[4] N. Yagiz Y. Z. Arslan, Y. Hacioglu. Prosthetic hand finger control using fuzzy sliding modes. *J Intell Robot System*, 52:121--138, 2008.

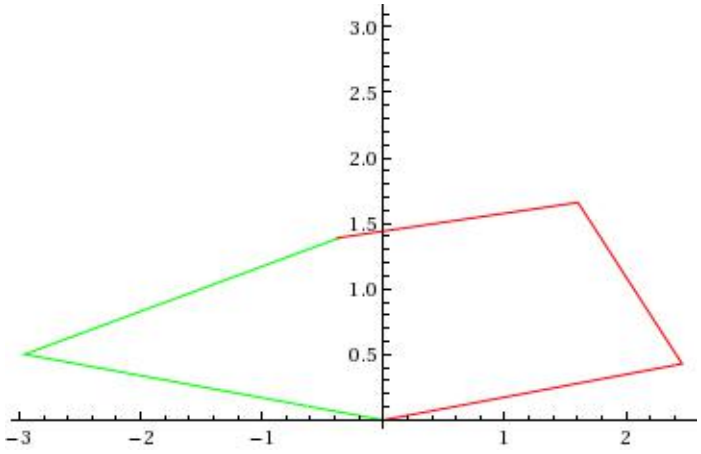

Figure 5: Finger and thumb touching.